**International Innovative Research Journal of Engineering and Technology**
Vol. 8, Issue. 1, Sep 2022, pp. 10~17
ISSN: 2456-1983, DOI: 10.32595/iirjet.org/v8i1.2022.161 

# Design for Removing Haze Utilizing the Light Scattering Model and Dark Channel Prior Approach

**Dhanasekaran Pachiyannan[1], Hoeun Lee[2]**
[1]Department of Electronics and Communication Engineering, The Kavery Engineering College, Mecheri, Salem, Tamilnadu-636453, India
[2]Department of Computer Science and Engineering, Konkuk University, Seoul, South Korea.

**Article Info**

***Article history:***

Received May 9, 2022
Revised Jul 12, 2022
Accepted Aug 11, 2022

***Keywords:***

Atmospheric scattering
Defogging algorithm
VLSI hardware
Atmospheric light scattering
Dark channel prior approach

**ABSTRACT**

The atmospheric scattering effect will cause the picture taken to become blurry and partially gray and white in the frog and hazy climate. Therefore, it is important to understand the defogging algorithm in these conditions. For object protection and detection, the haze reduction process—which is carried out before data processing—is essential. It recovers a clearer picture from a hazy source picture. The computational efficiency of the numerous haze removal techniques that have been presented has to be improved. In order to produce an improved output image by using a hazy source image, a straightforward and effective haze removal technique that is applicable to VLSI hardware design was developed in this study. It is dependent on the dark channel previous method as well as the natural light scatter model. This work extracts daylight from a whole image. This method starts with the atmospheric diffusion model and generates an estimated emission map using a dark channel before combining it with grayscale to create a revised transmission map. Here, an approach for estimating the local atmospheric light is used in the design to improve the output result, as opposed to depending on a single global atmospheric light enabling the reconstruction of the blurred scene. In the final, the design performs better in both qualitative and quantitative evaluations without distorting or overloading the colors. A six-stage VLSI design has been suggested for the method in order to modify this process for a real-time application.

***Corresponding Author:***

Dhanasekaran Pachiyannan,
Department of Electronics and Communication Engineering,
The Kavery Engineering College, Mecheri, Salem, Tamilnadu-636453, India.
Email: dhanawaves@gmail.com

## 1. INTRODUCTION

These days, embedded intelligence systems are becoming more and more necessary in outside surveillance systems, autonomous aerial aircraft, and sophisticated systems for driver assistance [1]. As technology advances, so does the extent to which humans can communicate with computers and various intelligent aid systems that enable humans to perform various activities more easily. For instance, cameras can be employed in intelligent transportation systems to recognize a vehicle for specific applications or to monitor streets or highways for the purpose of detecting traffic congestion [2]. In addition, the video feed from traffic monitoring systems might offer crucial details about an accident or collision, such as the license plate numbers of the vehicles involved. Due to air variation, haze significantly reduces image quality [3]. Intelligent systems may not function if a fuzzy image is not sufficiently visible. The dispersing of numerous suspended particles (such as fog, haze, smoke, and pollutants) in the environment typically degrades the visual quality of outdoor screens under fog and haze weather conditions. Haze is a typical natural phenomenon that drastically reduces contrast and alters an image's inherent color, especially when taken outside during bad weather [4].

Because fog relies on unknown scene depth information, haze removal is a difficult challenge. Image enhancement and image restoration are the two categories into which the existing haze removal techniques fall [5]. In this case, image enhancement eliminates the cause of the fog. This only applies to a wider extent. Information about the image will be lost. The physical procedure of imaging images under hazy conditions will be covered by image restoration. After that, a degraded model of the image will be created. The image quality will rise if the degrading process is reversed because a fog-free image free from degrading interference will be found. A hardware accelerator for removing haze from a single image was created in real-time. However, the outcomes of haze reduction were not on standards [6].

Haze reduction is typically accomplished by software that runs on CPU, DSP, and GPU. The implementation of these methods is hampered by lengthy computation durations and delays, which are significantly greater than the real-time demands. Parallel computation of the algorithm is simple. An effective ASIC is used to remove haze [7]. Due to their high power consumption and poor computing efficiency, the previously mentioned processors are not appropriate for mobile devices that require de-hazing. Therefore, in real-time embedded systems, a hardware implementation is essential.

To enhance the efficiency of the haze removal integrated system, an architecture for hardware based on dark channel prior (DCP) has been proposed to execute real-time haze removal. The atmospheric scattering model (ASM) is the basis for another kind of solution that is encouraged, and it produces great results by making full use of fresh data. Single-image haze removal has advanced significantly during the last few decades [8].

A hardware architecture based on DCP is suggested to carry out real-time haze removal in order to improve the performance of the haze removal embedded system. DCP is the most popular approach since it is easy to use and efficient. The advantages of the suggested hardware architecture are its low resource usage and high speed [9]. The ambient light measurement component is utilized in Alight computing. The picture restoration component is used to recover the de-hazing image. In the previous work, research created circuits for minimum and maximum computing, ambient light estimation, and scene recovery. In our earlier work, we created circuits for minimum and maximum computing, atmospheric light estimation, and scene recovery [10].

Multiple images of the same subject taken in various seasons are just not conceivable, despite the fact that there are many approaches that take advantage of varied accessible photographs. As a result, we decide to use a single image in the algorithm for defogging in our design [11].

## 2. LITERATURE REVIEW

[12] proposed hardware implementation for real-time haze removal. The process of haze reduction, which is done prior to data processing and is used to recover a sharper image from a foggy source image, is crucial for object recognition and avoidance. In order to produce a better output image from a foggy source image, a simple yet efficient haze removal technique that is relevant to VLSI hardware design has been developed in this study. In order to guarantee that the entire image is uniform without causing block difficulties, the local light estimation is dynamically modified based on the global light parameters. A hazy source image can be converted into a more polished output image by using the DCP technique. A six-stage transmitted system layout is recommended for the process to be executed for immediate analysis of full HD resolution (3840 × 2160) at 40 frames per second.

[13] introduced single image haze removal using dark channel prior. Haze removal is a common need in consumer/computational photography and computer vision applications. Removing haze can correct the color shift caused by the air light and significantly enhance scene perception. Most computer vision algorithms, ranging from simple picture analysis to complex object recognition, usually assume that the input image depicts the scene radiance. The dark channel before is a form of statistic for images taken outside without haze. Since the hazy imaging model assumes common transmission for all color channels, our method may not be able to reconstruct the true scene radiance of the distant objects, which would remain bluish.

[14] designed Fast image dehazing using improved dark channel prior. The physical method of imaging under hazy conditions is thoroughly examined in this work. The atmospheric scattering model is the starting point for the haze removal technique, which uses a dark channel prior to generating an approximated transmission map before combining it with grayscale to get a revised transmission map using a fast bilateral filter. The testing findings demonstrate substantial improvements in both computation performance and visual effect.

Ding et al [15] proposed that image dehazing and exposure using an enhanced atmospheric scattering model. The atmospheric scattering model is used to describe the interpretation of haze images. Through the incorporation of an additional parameter, the reflected light coefficient, into ASM, this study produces an improved ASM (EASM) that can more accurately simulate outside foggy scenes and address the

dull effect. Then, a simple yet effective grayworld-assumption-based technique called IDE is developed employing this EASM to enhance the visibility of fuzzy images. Tests reveal that EASM is more effective than ASM at modeling foggy images, and the resulting IDE performs better in terms of processing speed and recuperation clarity than most modern approaches.

[16] introduced VLSI implementation of and adaptive haze removal method. This work describes a very efficient real-time method that utilizes the DCP idea. The proposed method consists of three features: It first employs the local ambient light estimation to recover the object within different visibility ranges. Second, it dynamically refines localized solar radiation with global atmosphere light to avoid a block effect. Thirdly, it calculates the transmission map in a straightforward and efficient way. This demonstrates that it is a practical choice for haze removal to produce high-quality photos, qualifying it as a hardware type suitable for applications requiring immediate response.

## 3. PROPOSED METHODOLOGY

The Dark channel's earlier strategy works, as was already explained in the introduction. This approach, however, is unable to effectively manage the haze. The light scattering approach is used in this work to improve the transmission map. Figure 1 represents the proposed system flowchart.

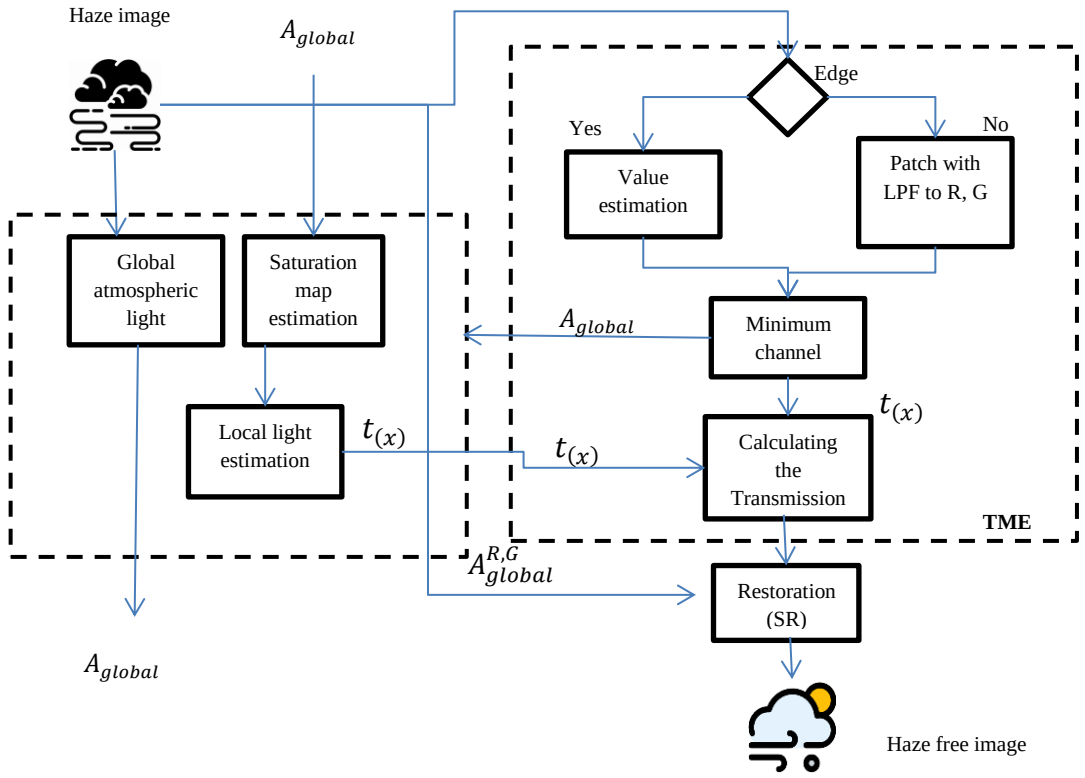


Figure 1. Flow chart for proposed system

This method consists of three main steps: transmission map estimation (TME), dynamic estimate of atmospheric light (DALE), and scene recovery (SR). The first phase is the DALE, where the total atmospheric light value $A_{global}$ is determined by identifying and keeping the pixel with the highest dark channel value.

$$K^e(y) = \frac{I^e(y) - A^e}{max[t(y)]} + A^c, \forall g \in R, G \qquad (1)$$

In the Equation (1), use a linear weighted approach to account for local ambient light, which may then be used to recreate the image. Therefore, in order for this method to work properly and calculate dynamic atmospheric light estimation, the image must be scanned twice. The estimation of transmission mapping is used in the second stage to identify the object's outlines. Ultimately, the image can be restored using the scene recovery process, which enters the transmission value and atmospheric light estimation into the following equation:

$$J(x) = \frac{I(y) - A}{[t(y)]} + A \qquad (2)$$

The Equation (2)'s entire procedure is described below. The atmospheric light represented by the letter "A" is crucial to the process of eliminating haze. The process of recovering the image that was rebuilt and estimating the transmission map both depend fundamentally on atmospheric light. The issue with this is that the black area would get significantly darker when the atmospheric light value increased.

The light section gets lighter as the environmental light value is lower. Therefore, in order to overcome the above problems, we apply the idea of dynamically evaluating the local light conditions for the purposes of this work. First, we must determine the overall atmospheric light value in order to maintain an initial level for the atmospheric light over the entire image. In order to keep the memory cost down, the technique used here uses a 3x3 patch size. After the process of estimating the global atmospheric light is finished, a flexible adjustment based on each patch's characteristics is suggested in order to improve the restoration process at every pixel. This is expressed as equation (3):

$$t_{(x)} = e^{\beta d(x)} \qquad (3)$$

A transmission map shows the rate at which light that is reflected by an item and impeded by haze or fog in a situation penetrates the environment and experiences exponential attenuation. It is simple to create the transmission map using the dark channel properties. More precisely, the previously discussed atmospheric light estimating process and the transmission map calculation are simple processes.

Transmission values in a local window must be assumed to be constant for estimation. Since the halo effect typically occurs at an object's contours, as we have shown above, we employ a method for detecting edges in order to reduce the number of halo artifacts. This design uses a 3x3 mask and a straightforward yet effective edge detection technique to keep the hardware low complexity. Transmission map estimation based on the Dark Channel Prior approximation can be shown as equation (4):

$$t(c) = 1 - \min_{c \in \Omega(c)} \left( \min_{c} \frac{Y^r(e)}{A^r} \right) \qquad (4)$$

From the above equation (4) the $A^c_{local}$ value and the transmission mapping value $t_c$ can be substituted to reconstruct the image $(c)$ following the inference of the local atmospheric light value and mapping for transmission.

The circuit shown in Figure 2 is composed of four parts: the storage buffer (MB), DALE, TME, and SR. The MB features a register bank (RB) unit and six line buffers (LBs) since each of the three primary color channels needs two.

Global atmospheric light calculation (GALC) and local atmospheric light calculation (LALC) are the two main units that make up this section. Calculating appropriately suitable light conditions for the foggy image is the primary purpose of the DALE component.

The figure shows the construction of this unit, which is used to measure ambient light. The dark channel in stage 2 is determined by the patch values that were acquired from RB. In stage 3, the temporary maximum value $max_{(t)}$ is either retained or substituted based on a comparison with the dark channel number from stage 2.

$$J(x) = \frac{I(x) - \hat{\mathrm{A}}}{max\big(\hat{\mathrm{s}}(x)\big)} + A \qquad (5)$$

This unit, whose design is shown in Figure, is used to modify global atmospheric light in order to achieve an appropriate local value determined by the patch feature. The worldwide atmospheric light minimum is established in step 2. In stage three, the atmospheric light of the dark portion and the dark threshold are created. An approximation technique that makes use of the Euclidean algorithm has been used to lessen computational complexity in order to minimize division operations.

The diagram above shows the hardware architecture of the TME component. This TME section includes units for transformation calculation (TC), modified dark channel computation (MDCC), and three-channel edge detection (TCED). The MDCC unit includes both a standard dark channel computation and a margin dark transmit calculation, which employs the center pixel's beginning values. The equation (6) below expresses this.

$$t(c) = 1 - \min_{y \in \Omega(c)} \left( \min_{c} \frac{Y^r(e)}{A^r} \right) + t(c). \min_{y \in \Omega(c)} \left( \min_{c} \frac{Y^r(e)}{A^r} \right) \qquad (6)$$

The multiplicative term (direct transmission) in the hazy imaging model must be removed using the dark channel prior to equation (6) above. There is just the additive term remaining. Compared to earlier single-image haze reduction techniques that mostly relied on the multiplicative term, this approach is entirely different.

The hardware architecture of the restoration unit, which is the only unit in this section, is displayed in Fig. 3.6. The LUT in the TE section provides the 1/t number from the look-up table. The 1/t is an expansion of (I-A) according to Stage 5. Additionally, the final values are shifted 8 bits to the left to eliminate the decimal in order to match the LUT's precision. The output pixels are arranged in the same sequence as the input pixels, from the left-top corner to the right-bottom corner, to produce the restored image in raw image format for storage and display. Equation (7) provides an expression for this.

$$t(u,v) = \frac{Y_{(e,R_0)}}{Y_{(e,R_1)}} \qquad (7)$$

In order to calculate the function from the observed images, which serve as the observation for calculating $R_0$ and $R_1$ from the preceding equation, $t(u,v)$is created as the ratio of two corresponding frequency components from two observations, i.e., $t(u,v)$.

Multiple frame estimation produces consistent findings as the number of frames passes six, even though two-frame estimations vary depending on the frames employed.

## 4. RESULT AND DISCUSSION

The proposed research was evaluated both qualitatively and quantitatively to confirm its efficacy. The two experiments carried performed on the benchmark photos are described in this section after the DPI utilized in the investigation. In the first experiment, a constant variable in ADCP was used, while in the second experiment, optimum parameters were found using the ACO method. A suitable DPI is necessary in order to evaluate the image-removing hazing effect quantitatively. Consequently, $DPI_\delta$is described as

$$DPI_\delta = \frac{b_i - b_0}{b_0} \qquad (8)$$

Here the numerical values of edges in hazy and de-hazed photos are denoted by the letters $b_i$ and no, respectively. Because this technique is meant to eliminate spatially invariant haze, it can only eliminate a tiny layer of haze that corresponds to the closest objects when the image's depth is not constant. The de-hazing effect increases with the $DPI_\delta$. This DPI's clear flaw, though, is that it ignores the impact of distortion on a dehazed image.

The following outcomes are obtained by utilizing Xilinx ISE for the VLSI implementation and the iSim simulator for simulation. Following the processing of the RGB data for the GALC, LALC, TM, and SR stages, the output is displayed in the following figures.

The fixed point number format is used for all mathematical operations in our hardware architecture. A low-cost approximation method is used to calculate α. Additionally, we obtain the reciprocal of t(x) using a lookup table instead of a more costly divider. It goes without saying that the lower-complexity approximation methods will degrade the defogging effects.

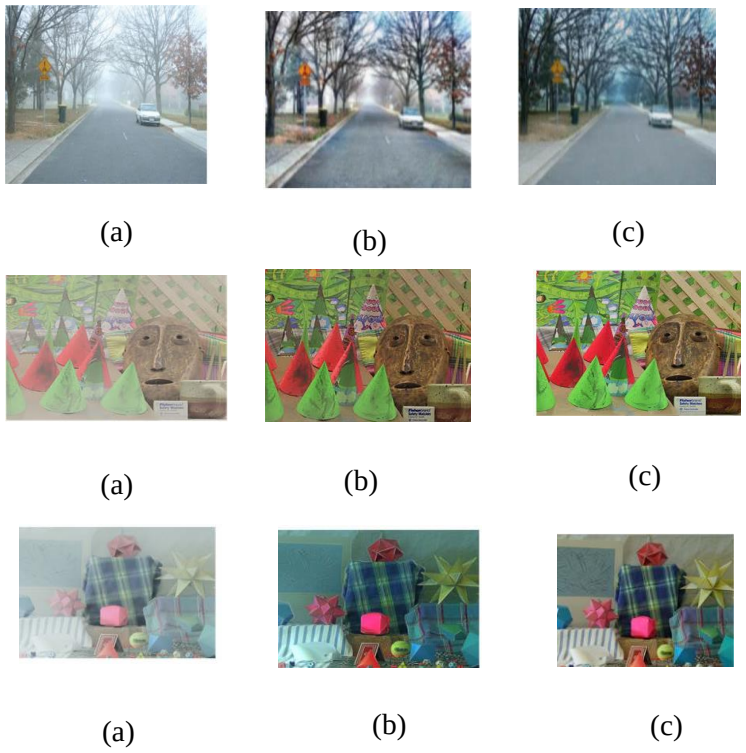


Figure 2. Comparison of input and output image after de-hazing

The output of the de-hazing procedure, which eliminates the fog or haze from the image, is shown in the above figure. The input image is indicated by the (a) in Figure 2 above. The output of the prior paper is shown in (b), while the output of the suggested system is shown in (c). The underestimate of dark channels in regions with depth discontinuities was the origin of these artifacts. However, the halo artifacts produced during dehazing can be successfully reduced with DCP, making photos appear sharper. Images in the third column indicate that haze effects can be lessened by using DCP with a constant setting. The findings in the fourth column showed that ADCP may more successfully prevent the development of halo artifacts in the photos when its parameter is improved. In picture dehazing, the suggested technique can successfully avoid haze generation as long as the dehazing ability is unchanged. As long as the removing hazing effect, as well as color distortion, were taken into consideration, the experimental findings show that DCP with optimum parameters produced the best dehazing outcome.

Table 1. Comparison of images execution time

| Images | Image size | Previous method | Our method |
|---|---|---|---|
| Road and trees | 463*533 | 4.034 | 0.0064554 |
| Toys | 346*458 | 5.645 | 0.0002145 |
| Gifts | 454*576 | 7.345 | 0.003244 |

Table 1 lists the computation times for the images of roads, trees, toys, and gifts. The DPI findings based on Fig. 2 are displayed in Table 1. The second and third columns display the evaluation findings of $DPI_{\delta}$, which demonstrate that the DCP-based method generally yields better results. Consequently, the proposed method can remove most of the haze effect and has improved de-hazing performance, revealing more edge information. The DCP-based dehazing approach yielded a superior result than the DCP-based dehazing method, suggesting that the proposed method successfully avoids color changes that would otherwise occur during image dehazing in addition to effectively removing haze.

Table 2. Overview of device use

| Logic Utilization | Used | Available | Utilization |
|---|---|---|---|
| Quantity of slices LUT's | 456 | 345331 | 03% |
| Number of bonded | 565 | 2163432 | 0% |

| | | | |
|---|---|---|---|
| COBs | | | |
| DSP | 342 | 12354 | 64% |
| Fully utilized LUT number | 435 | 656 | 32% |
| BUFG number | 767 | 4321 | 03% |
| Slice register | 646 | 19 | 82% |

The area report of the used summary, which can be utilized in the estimated outcome image, is shown in table 2.

Table 3. Improving the parameters that were acquired by light scattering

| **Images** | **Parameters** | | |
|---|---|---|---|
| | $g_s$ | $g_\sigma$ | λ |
| Trees | 5346 | 3 | 3.2 |
| Dolls | 2355 | 8 | 2.5 |
| Street | 5623 | 4 | 8.0 |
| Rail | 6534 | 5 | 4.6 |
| Roads | 2387 | 3 | 6.4 |
| Gifts | 2359 | 4 | 9.6 |

The optimal parameters acquired for the various photos are displayed in Table 3. Figure 2 displays the hazy image in the first column, the DCP-dehazed images in the second column, the DCP-dehazed images with a constant parameter, and the DCP-dehazed images with TME, SR, etc. in the final column.

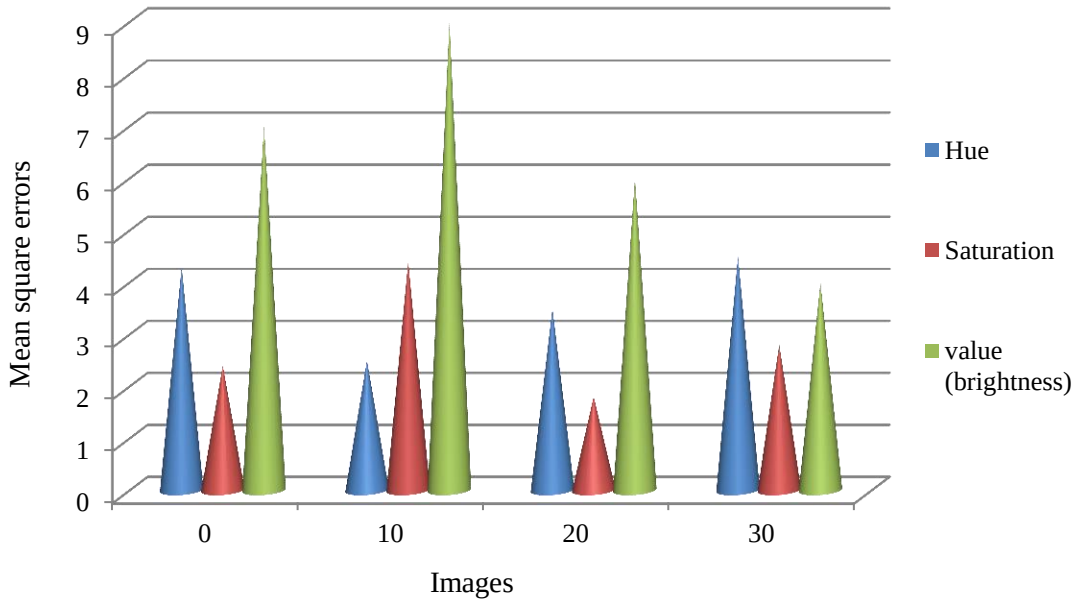


Figure 3. Quality analysis

From Figure 3, MSE is assessed for both clear and fuzzy images in the H, S, and V channels. It is clear that the presence of haze has a considerable impact on the V channel. The ability to recognize and differentiate originally bright areas of the image from foggy areas is another essential feature of the V channel.

## 5. CONCLUSION

This study presents a dark channel prior method-based real-time and extremely efficient VLSI architecture. Architecture for hardware was created and implemented in usage. The hardware architecture performs well and is quite efficient. Even for huge photos, it met the real-time requirement and produced

good image recovery results. This algorithm can create more vibrant photos without sacrificing the contrast between the dark and bright areas. Three features make up the suggested approach: In order to bring the object back into various visibility ranges, it first uses the local ambient light estimation. In haze removal photos, the contrast is improved and the halo effects are avoided. The experimental findings demonstrate that the suggested approach produces exceptional dehazing outcomes. As a result, an image captured under such circumstances will have less contrast and considerably softer color, which will lower the physical integrity of the objects in the picture and further affect the quality of any processing programs that use this data. In addition, a six-stage pipelined hardware design is suggested to carry out the procedure and process full HD quality (1920 × 1080) in real-time at 40 frames per second. This is quick enough to satisfy the necessary standards. This indicates that it is a viable option for haze removal in order to provide high-quality images, making it a type of hardware that can be used in real-time applications.

**REFERENCES**


[1] Sharma, T., Shah, T., Verma, N. K., & Vasikarla, S. (2020, October). A review on image dehazing algorithms for vision based applications in outdoor environment. In *2020 IEEE Applied Imagery Pattern Recognition Workshop (AIPR)* (pp. 1-13). IEEE.

[2] Zhang, B., & Zhao, J. (2016). Hardware implementation for real-time haze removal. *IEEE Transactions on Very Large Scale Integration (VLSI) Systems*, *25*(3), 1188-1192.

[3] Shiau, Y. H., Yang, H. Y., Chen, P. Y., & Chuang, Y. Z. (2013). Hardware implementation of a fast and efficient haze removal method. *IEEE Transactions on Circuits and Systems for Video Technology*, *23*(8), 1369-1374.

[4] Liang, Z., Liu, H., Zhang, B., & Wang, B. (2014). Real-time hardware accelerator for single image haze removal using dark channel prior and guided filter. *IEICE Electronics Express*, *11*(24), 20141002-20141002.

[5] Cheng, W. C., Hsiao, H. C., Huang, W. L., & Hsieh, C. H. (2020). Image Haze Removal Using Dark Channel Prior Technology with Adaptive Mask Size. *Sensors & Materials*, *32*.

[6] Li, B., Hua, Y., & Lu, M. (2021). Advanced multiple linear regression based dark channel prior applied on dehazing image and generating synthetic haze. *arXiv preprint arXiv:2103.07065*.

[7] Zhu, J., Meng, L., Wu, W., Choi, D., & Ni, J. (2021). Generative adversarial network-based atmospheric scattering model for image dehazing. *Digital Communications and Networks*, *7*(2), 178-186.

[8] Peng, Y. T., Lu, Z., Cheng, F. C., Zheng, Y., & Huang, S. C. (2019). Image haze removal using airlight white correction, local light filter, and aerial perspective prior. *IEEE Transactions on Circuits and Systems for Video Technology*, *30*(5), 1385-1395.

[9] Chang, H. Y., Hsu, C. C., & Lee, Y. H. (2020, September). Smooth dark channel prior technique for image dehazing applications. In *2020 IEEE International Conference on Consumer Electronics-Taiwan (ICCE-Taiwan)* (pp. 1-2). IEEE.

[10] Bhola, A., Sharma, T., & Verma, N. K. (2021). DCNet: Dark Channel Network for single-image dehazing. *Machine vision and applications*, *32*(3), 62.

[11] Ganguly, B., Bhattacharya, A., Srivastava, A., Dey, D., & Munshi, S. (2021). Single image haze removal with haze map optimization for various haze concentrations. *IEEE Transactions on Circuits and Systems for Video Technology*, *32*(1), 286-301.

[12] Zhang, B., & Zhao, J. (2016). Hardware implementation for real-time haze removal. *IEEE Transactions on Very Large Scale Integration (VLSI) Systems*, *25*(3), 1188-1192.

[13] He, K., Sun, J., & Tang, X. (2010). Single image haze removal using dark channel prior. *IEEE transactions on pattern analysis and machine intelligence*, *33*(12), 2341-2353

[14] Xu, H., Guo, J., Liu, Q., & Ye, L. (2012, March). Fast image dehazing using improved dark channel prior. In *2012 IEEE international conference on information science and technology* (pp. 663-667). IEEE.

[15] Ju, M., Ding, C., Ren, W., Yang, Y., Zhang, D., & Guo, Y. J. (2021). IDE: Image dehazing and exposure using an enhanced atmospheric scattering model. *IEEE Transactions on Image Processing*, *30*, 2180-2192.

[16] Kuo, Y. T., Chen, W. T., Chen, P. Y., & Li, C. H. (2019). VLSI implementation for an adaptive haze removal method. *IEEE Access*, *7*, 173977-173988.